The Indian Journal of Pediatrics (September 2018) 85(9):729–737
https://doi.org/10.1007/s12098-017-2592-x

ORIGINAL ARTICLE

Prenatal and Postnatal Diagnosis of Rhabdomyomas and Tuberous Sclerosis Complex by Ultrafast and Standard MRI

Ying Zhou[1] · Su-Zhen Dong[1] · Yu-Min Zhong[1] · Ai-Min Sun[1]

Received: 27 May 2017 / Accepted: 19 December 2017 / Published online: 9 January 2018

Abstract

Objective To examine the features of cardiac rhabdomyomas and tuberous sclerosis in fetuses and infants using magnetic resonance imaging (MRI) and to determine whether MRI is an effective tool to facilitate early detection of tuberous sclerosis complex (TSC).

Methods Fifteen patients with TSC were evaluated by ultrafast or standard MRI between June 2005 and September 2016. Fifteen patients were divided into two groups. Group A included five cases in utero and followed in infancy with gestational ages from 26 + 1 to 38 + 2 wk. Group B included ten cases aged from 36 d to 18-mo-old.

Results There were 11 and 10 cardiac lesions of prenatal and postnatal period respectively in five subjects of Group A and 27 cardiac lesions in ten subjects of Group B. There were more than 31 prenatal brain lesions and 30 postnatal brain lesions in Group A and 169 lesions in Group B. Standard postnatal brain MRI confirmed the prenatal study of Group A. At 1 y follow up of Group A, there was partial regression of 2 cardiac lesions, complete regression of 1 cardiac lesion, no obvious regression of 8 cardiac lesions.

Conclusions When one or multiple cardiac tumors are detected by ultrasound in fetal period or some specific clinical manifestations are presented in infancy, fetal ultrafast MRI or standard MRI is suggested to make early diagnosis of TSC.

Keywords MRI · Rhabdomyomas · Tuberous sclerosis · Central nervous system · Fetus · Infant

Introduction

Tuberous sclerosis complex (TSC) is a neurocutaneous syndrome with autosomal dominant inheritance that variably affects the brain (approximately 50%), skin (50%), heart (30%), kidneys (11%), and any other organ system [1, 2]. The coincidence of cardiac rhabdomyomas and tuberous sclerosis was first described in 1862 in a newborn. Obvious signs can appear early in the perinatal period. Prenatal screening of fetuses of mothers affected with TSC using ultrasound (US) is effective for detecting cardiac rhabdomyomas [3–5]; however, previous studies often faced difficulties in reaching the diagnosis of tuberous sclerosis of brain lesions in fetal and infantile age groups because US is not sensitive for evaluation of lesions of the brain. MRI is a particularly reliable adjunct to decide the extent of cerebral involvements in TSC and can also identify cardiac lesions detected by US [6–9]. Herein, authors reviewed retrospectively the extensive work up incorporating both fetal ultrafast (5 cases of Group A) and postnatal standard MRI images of 15 patients (5 cases of Group A and 10 cases of Group B) with cardiac rhabdomyomas and tuberous sclerosis.

Material and Methods

Between June 2005 and September 2016, seven pregnant mothers with prenatal US suggesting cardiac tumors were referred from local hospitals to authors' institution for prenatal MRI evaluations. All patients provided informed consents before the examination. Two of seven cases were excluded from entry into the study due to absence of cardiac and brain abnormalities after MRI examination and they were continuously followed up by local US. Gestational ages of the five remaining cases were 34 + 1, 33 + 5, 37 + 2, 38 + 2 and 26 + 1 wk respectively determined by local US reports. All five cases received correlated follow-up images within 1 y after birth.

✉ Su-Zhen Dong
dongsuzhen@126.com

[1] Department of Radiology, Shanghai Children's Medical Center, 1678 Dongfang Rd., Shanghai 200127, China

Between June 2005 and September 2016, 10 neonatal and infantile patients had cardiac MRI results suggestive of cardiac rhabdomyomas and brain MRI identified as having multiple subependymal nodules, subcortical white matter, or cortical tubers. Ages were from 36 d to 18-mo-old.

Ten patients were referred to authors' institution due to the clinical manifestations and were included in Group B: 1 patient presented with skin depigmentation, 1 patient presented with arrhythmia, 2 patients presented with arrhythmia and physical retardation, 5 patients presented with arrhythmia and epilepsy, 1 patient presented with skin depigmentation and arrhythmia. No prenatal data of these ten patients was provided.

The diagnosis standard for TSC is established based on two major features or one major plus more than two minor features (The second International TSC Consensus Conference, TSCCC, 2012) [10]. The TSCCC criteria is also applied to fetal MRI [11].

MRI was performed with two 1.5 T units, (Signa, GE Medical Systems, Milwaukee, WI, USA; Achieva Nova dual, PHILIPS Medical Systems, Best, Netherlands) and a brain coil or an eight-channel, phased array cardiac coil. As the retrospective work was done using two MRI machines with different vendors, authors summarized the fetal MRI sequences and parameters of different MRI machines with three major manufacturers included ultrafast T2-weighted spin echo; balanced gradient echo, and T1-weighted sequence (Table 1) 3 to 4 mm slices thickness, with a gap of 1–2 mm or not. Patients were placed in a supine, feet-first position in the magnet in order to minimize claustrophobia.

Patients undergoing standard brain and cardiac MRI examinations were placed in a supine, head-first position in the magnet. Standard brain imaging sequences included a spin-echo T1-weighted sequence (T1WI, repetition time/echo time, 450 ms/13 ms), a T2-weighted sequence (T2WI, 3225 ms/100 ms). Section thickness was, 5 mm; with a gap of 1–2 mm or not; Standard cardiac imaging sequences included an oblique balanced gradient echo sequence and a contrast enhanced MR angiography (MRA) sequence; the MRA images were reconstructed by maximal intensity projection on the work station, a conventional section thickness was 5 mm, with a gap of 1–2 mm or not.

Standard brain MRI, cardiac MRI and ultrafast fetal MRI duration averaged approximately 20 min, 40 min and an hour respectively, Sedatives and intravenous gadolinium-based contrast were only used in brain and cardiac examinations of infants.

All of the MR images were reviewed cooperatively by three radiologists (ZY, SZD and YMZ). The specialties of these three evaluating radiologists are all fetal and pediatric imaging diagnosis, they have dedicated to this field for more than 10 to 20 y. The clinical manifestations and US results were known at the time of acquisition and when the MR images were interpreted.

Results

In the five fetuses from local hospitals which suggested cardiac tumors by prenatal US (Group A), both brain nodules and cardiac lesions were detected by ultrafast MRI. Clinical features, gestational age at US diagnosis, fetal US record, prenatal and postnatal MRI outcomes of Group A are shown in Table 2.

The data from ten patients of Group B (age at diagnosis, sex, clinical presentation, cerebral and cardiac imaging features) are presented in Table 3.

There were more than 31 prenatal brain lesions (24 subependymal nodules and 7 subcortical and cortical tubers) in Group A. Ultrafast fetal MRI detected subependymal nodules in all five fetuses and additional cerebral cortical and subcortical lesions in one patient from Group A; lesion signals were hyperintense on T1 weighted sequences (Fig. 1a, *white arrow*) and hypointense on T2 weighted sequences (Fig. 1b, *black arrows*) with respect to normal white matter. Lesion sizes were 2-5 mm. Within 1 y follow-up, there were 30 postnatal brain lesions (18 subependymal nodules and 12 subcortical and cortical tubers) in Group A, lesion sizes were 2-6 mm. Similar to the fetal MR exams, postnatal MR exams showed subependymal nodules in all five subjects. However, cortical and subcortical lesions were more commonly detected compared to the fetal MRI (Fig. 2a and b, *white arrow*). One

Table 1 Vendor specific sequence parameters for 1.5 T fetal MR

Sequence	GE	PHILIPS	SIEMENS
Balanced gradient echo	Fast imaging employing steady-state acquisition (FIESTA) [TR/TE:4.0 ms/2 ms]	Balanced fast field echo (B-FFE) [TR/TE:3.6 ms/1.8 ms]	True fast image with steady-state precession (True FISP) [TR/TE:10 ms/3 ms]
Ultra fast T2-weighted spin echo	Multi-planar single-shot fast spin echo (SS-FSE) [TR/TE:1300 ms/90 ms]	Single-shot turbo spin-echo (SS-TSE) [TR/TE:12,000 ms/80 ms]	Half Fourier Single Shot Turbo fast spin echo (HASTE) [TR/TE:1500 ms/95 ms]
T1-weighted	Fast inversion recovery motion intensive (FIRM) [TR/TE:10 ms/5 ms]	Short T1 inversion recovery TFE (T1- TFE) [TR/TE:15 ms/7 ms]	Inversion Recovery Turbo Spin Echo (IR-TSE) [TR/TE:10 ms/5 ms]

Table 2 Imaging findings of five fetuses in Group A

Case	Gestational age (GA) & gender	Fetal US	Prenatal MRI		Postnatal MRI	
			Cerebral lesions Location Number Maximal size	Cardiac tumor Location Maximal size	Cerebral lesions Location Number Maximal size	Cardiac tumor Location Maximal size
1	34 wk	RV tumor	S	Multiple	S; SWM; C	Multiple
	M		More than 3 lesions	LA; LVS*; RV; LV	9 lesions	LAFW; LVFW; RVFW
			2 mm	7 mm	2 mm	7 mm
2	33 wk	Cardiac tumor	S	Multiple	S; SWM;C	Multiple
	M		More than 6 lesions	RVS; LV	5 lesions	LVFW; RVS
			5 mm	10 mm	3 mm	5 mm
3	37 wk	Multiple cardiac tumors	S	Single	S; SWM	Single
	F		More than 9 lesions	RV	7 lesions	RVFW•
			4 mm	6 mm	3 mm	3 mm
4	38 wk	Multiple cardiac tumors	S	Multiple	S	Multiple
	F		More than 3 lesions	RV*; LVS	3 lesions	RVFW; LVS
			5 mm	8 mm	6 mm	8 mm
5	26 wk	RV tumor	S; SWM; C	Multiple	S; SWM; C	Multiple
	M		More than 10 lesions	RV; LV	6 lesions	RVFW; LVS
			3 mm	5 mm	3 mm	5 mm
Total			More than 31 lesions	11 lesions	30 lesions	10 lesions

M Male; *F* Female; *S* Subependyma; *SWM* Subcortical white matter; *C* Cortex; *LA* Left atrium; *RV* Right ventricle; *LV* Left ventricle; *LAFW* Left atrial free wall; *LVS* Left ventricular septum; *LVFW* Left ventricular free wall; *RVFW* Right ventricular free wall; *RVS* Right ventricular septum

*Cardiac lesions regressed

• Cardiac lesion reduced

patient had isolated subependymal nodules on both the pre and postnatal MR scans.

In Group A, 11 cardiac tumors were detected in utero. Ultrafast fetal MRI detected multiple cardiac lesions in four fetuses and a single cardiac tumor in one patient (Fig. 1c, d and e, *white arrow*) from Group A; 3/11 lesions were located in the ventricular septum. Seven of the eleven lesions were located in the right or left ventricle. One of the eleven lesions was located in the left atria; lesion signals were isointense on both T1 weighted sequences and T2 weighted sequences with respect to myocardium. Lesion sizes ranged from 5 to 10 mm. Within 1 y follow up, there was partial regression of 2/11 lesions (Fig. 2c, *black arrow*), (Fig. 2d), complete regression of 1/11 lesions, and 8 lesions had no obvious regression.

One fetus had multiple renal lesions detected by fetal ultrafast MRI which was not mentioned by fetal US. Standard MRI confirmed the renal lesions after birth.

There were 169 brain lesions (58 subependymal nodules and 111 subcortical or cortical tubers) detected in Group B. Standard brain MRI detected subependymal nodules in nine patients and additional cerebral cortical and/or subcortical lesions in seven patients from Group B; lesion signals were isointense or hyperintense on T1 weighted sequences and hyperintense or hypointense on T2 weighted sequences with respect to normal white matter. Lesion sizes were between 3 and 12 mm. Seven of the ten patients of subcortical white matter or cortical tubers characteristic on MRI varied according to the progression of myelination of the first year of life: 3/7 (between 34 d and 4 mo) were hyperintense on T1-weighted sequence and hypointense on T2-weighted sequence, while 4/7 (aged between 11 and 18 mo) were hypointense on T1-weighted sequence and hyperintense on T2-weighted sequence with respect to the white matter.

Twenty seven cardiac tumors were detected in ten infants of Group B over the study period. Standard cardiac MRI detected multiple cardiac lesions in seven patients and a single cardiac tumor in three patients from Group B (Fig. 3a, *white arrow*; Fig. 3b, *black arrow*). Furthermore, 11/27 cardiac lesions were located in the ventricular septum, 16/27 were located in the ventricular free wall. Five of the twenty seven lesions caused outflow tract obstruction (Fig. 4a, *white* and *black arrow*), 2/5 were located in the left ventricular outflow tract (Fig. 4b, *white arrow*), (Fig. 4c, *black arrow*), 2/5 were located in the right ventricular septum (Fig. 4d, *black* and *white arrow*), 1/5 was located in left ventricular free wall. Tumor sizes ranged from 3 to 15 mm. Tumor signals were isointense on both T1 weighted sequences and T2 weighted sequences to myocardium.

Table 3 Clinical features, MRI findings of ten infants (postnatal exams) of Group B

Case	Age	Gender	Presentation	Cerebral lesions Location Number Maximal size	Cardiac tumor Location (Number) Maximal size
1	12 mo	M	Skin depigmentation	S; SWM; C	Multiple
				15 lesions	RVS (1); RVFW(2); LVFW(2)
				8 mm	15 mm
2	13 mo	M	Epilepsy	S;	Multiple
				2 lesions	LVOT*(1); LVFW(1)
				4 mm	12 mm
3	18 mo	M	Physical retardation	S; SWM; C	Single
				35 lesions	LVOT*(1)
				6 mm	12 mm
4	34 d	M	Skin depigmentation	S; SWM; C	Multiple
				43 lesions	RVFW(1); LVS(1); RVS(1)
				12 mm	10 mm
5	7 mo	F	Epilepsy	S;	Single
				7 lesions	RVS(1)
				4 mm	9 mm
6	1 mo	F	Epilepsy	SWM; C	Single
				6 lesions	LVOT(1)
				4 mm	13 mm
7	11 mo	M	Physical retardation	S; SWM; C	Multiple
				25 lesions	RVS*(2); LVS(1); LVFW*(1)
				8 mm	14 mm
8	4 mo	M	Epilepsy	S; SWM; C	Multiple
				15 lesions	LVFW(1); RVS(1); RVOT(2)
				7 mm	13 mm
9	18 mo	M	Arrhythmia Epilepsy	S; SWM; C	Multiple
				18 lesions	LVS(1); LVFW(1)
				6 mm	10 mm
10	47 d	F	Prenatal US suggested cardiac tumors, no prenatal MRI	S;	Multiple
				3 lesions	RVFW(1); LVFW(1); RVS(1); LVS(1)
				3 mm	3 mm
Total				169 lesions	27 lesions

M Male; *F* Female; *S* Subependyma; *SWM* Subcortical whitematter; *C* Cortex; *LVOT* Left ventricle outflow tract; *RVOT* Right ventricle outflow tract; *RVS* Right ventricular septum; *LVS* Left ventricular septum; *RVFW* Right ventricular free wall; *LVFW* Left ventricular free wall

*Variable development of intracardiac flow obstruction

Discussion

Tuberous sclerosis complex (TSC) is a cellular differentiation and proliferation disorder. Abnormal neuronal migration plays a major role in the neurological dysfunction seen in this condition [12]. Three different mutations located on chromosomes 9, 11 and 16 have been associated with the disorder [13]. A definitive diagnosis of TSC is initially made according to the diagnostic TSCCC criteria put forth by Roach et al. in 1998. Cardiac rhabdomyomas and subependymal nodules are two major criteria, which constitute a definitive diagnosis of TSC. The 2012 International Tuberous Sclerosis Complex Diagnostic Criteria provided current and updated definitions using best available evidence (genetic diagnostic criteria and clinical diagnostic criteria) to establish the diagnosis of TSC in affected individuals [10].

Rhabdomyomas are the most common primary cardiac tumors in both prenatal and neonatal periods [14]. Prenatally, cardiac rhabdomyomas are strong predictors of TSC [15]. The available literature states that the cardiac tumors tend to involute with no malignant potential [16, 17], but they also can be associated with life-threatening complications [18] such as

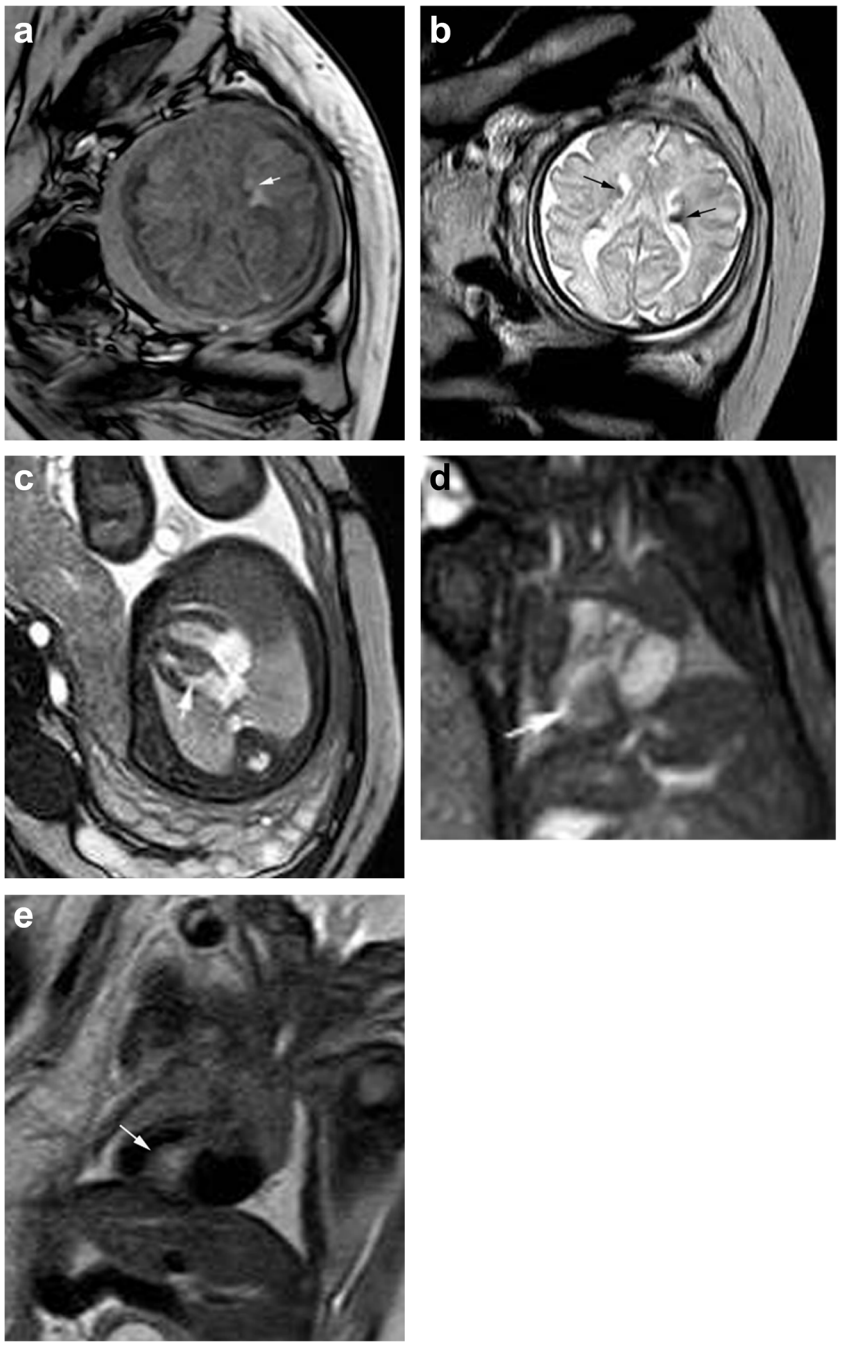

Fig. 1 Prenatal MR images of a patient of Group A at 33 wk' gestation; (**a**, **b**) Bilateral subependymal multiple nodules. Lesion signals were hyperintense on T1 weighted sequences (**a**, *white arrow*) and hypointense on balanced gradient echo sequence (**b**, *black arrows*) with respect to normal white matter. **c**, **d** Transverse and coronal balanced gradient echo sequences show a rhabdomyoma adherent to the left ventricular septum, tumor signal was isointense to myocardium. (*white arrow*). **e** A coronal balanced gradient echo sequence reveals this rhabdomyoma (*white arrow*)

fetal hydrops, arrhythmia, intracardiac flow obstruction, and atrioventricular valve dysfunction. The presenting symptoms for 9 of the cases in Group B included arrhythmia. Three risk factors are associated with tuberous sclerosis: rhabdomyoma size, isolated or multiple cardiac lesions, and family history of tuberous sclerosis [19]. Multiple cardiac tumors usually reflect a more severely afflicted heart. Size and location are also related to the risk for complications. Fetal US is able to detect cardiac lesions, but MRI is capable of assisting in tissue characterization by applying different sequences and helping define the relationship with normal structures. In the index study, fetal MRI detected one or more cardiac lesions in all patients, and provided the size and location of these lesions. Standard postnatal cardiac MRI also detected cardiac lesions in all patients. Table 2 shows that there are no obvious differences in sensitivity between fetal and standard postnatal MRI with regard to the location, size, and number of brain and cardiac lesions. Furthermore, Standard postnatal cardiac MRI also detected cardiac lesions in all patients, 5 of which caused variable hemodynamic obstructions that gave additional diagnostic information to the investigating radiologists. Currently, further advances in MRI sequencing technology facilitate fetal

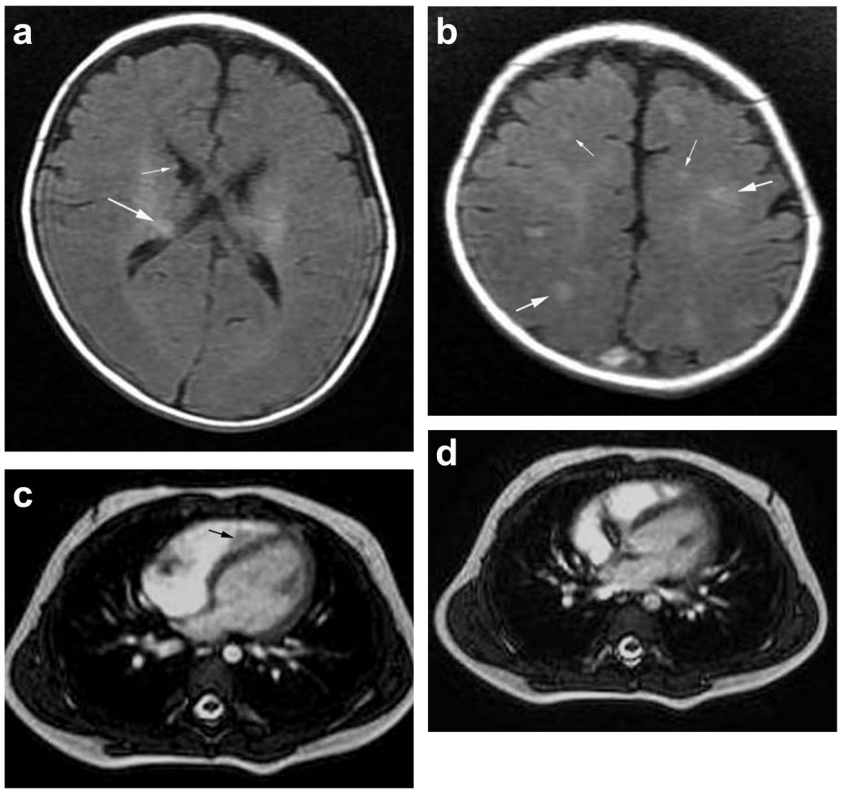

Fig. 2 Postnatal MRI images of Fig. 1 patient, 6-mo-old, female; (**a**, **b**) a transverse spin echo T1-weighted brain MRI sequence displays subependymal nodules, bilateral frontal and parietal subcortical white matter and cortical tubers (*white arrows*). Lesion signals were hyperintense with respect to normal white matter. **c**, **d** A transverse balanced gradient echo sequence shows the rhabdomyoma adherent to the left ventricular septum regressed (*black arrow*)

cardiac imaging by improving soft tissue contrast and better lesion detection.

When cardiac lesions are detected in the fetus, brain MRI is required. The coincidence of tuberous sclerosis and rhabdomyomas in patients had been underestimated until MRI techniques allowed the non-invasive investigation of the entire fetus [20]. US is acknowledged as the primary imaging modality for evaluating cardiac tumors, however, previous studies often faced difficulties in reaching the diagnosis of tuberous sclerosis of brain lesions in the fetus as US is not very sensitive for evaluation for tubers. Moreover, US has some difficulties in differentiating subependymal nodules from hemorrhage or heterotopia. Ultrafast MRI sequences for fetuses and standard MRI for infants, have proved to be of particularly reliable value in the evaluation of subjects. MRI is distinguished by its superior sensitivity and specificity compared to US and lack of radiation compared to computed tomography. MRI can also provide images in all planes without repositioning the patient and it can determine whether other organs are involved [21].

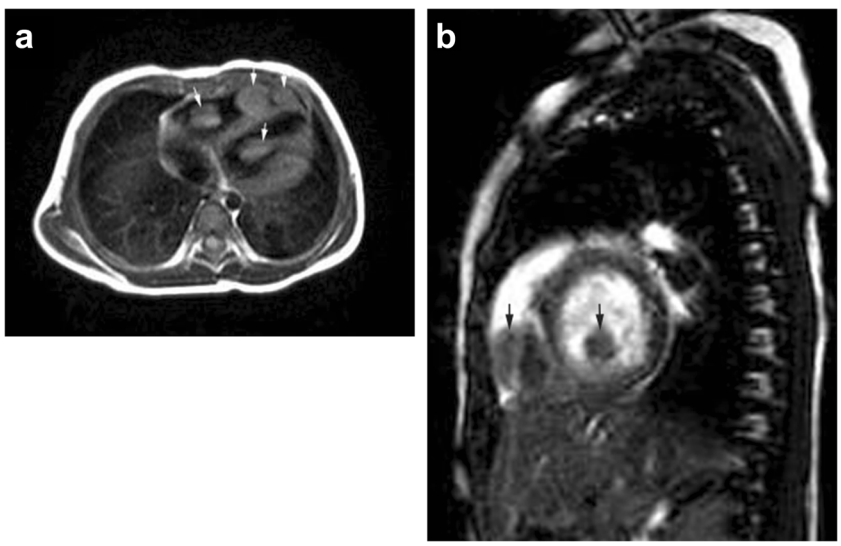

Fig. 3 Cardiac MR images of a boy of Group B at 12-mo-old; (**a**) A transverse spin echo T1-weighted sequence show multiple rhabdomyomas in the right ventricular septum, right ventricular free wall, and left ventricular free wall, tumor signals were isointense to myocardium (*white arrows*). **b** A sagittal balanced gradient echo sequence shows two round rhabdomyomas in the right ventricular free wall and left ventricular free wall (*black arrows*), tumor signals were isointense to myocardium

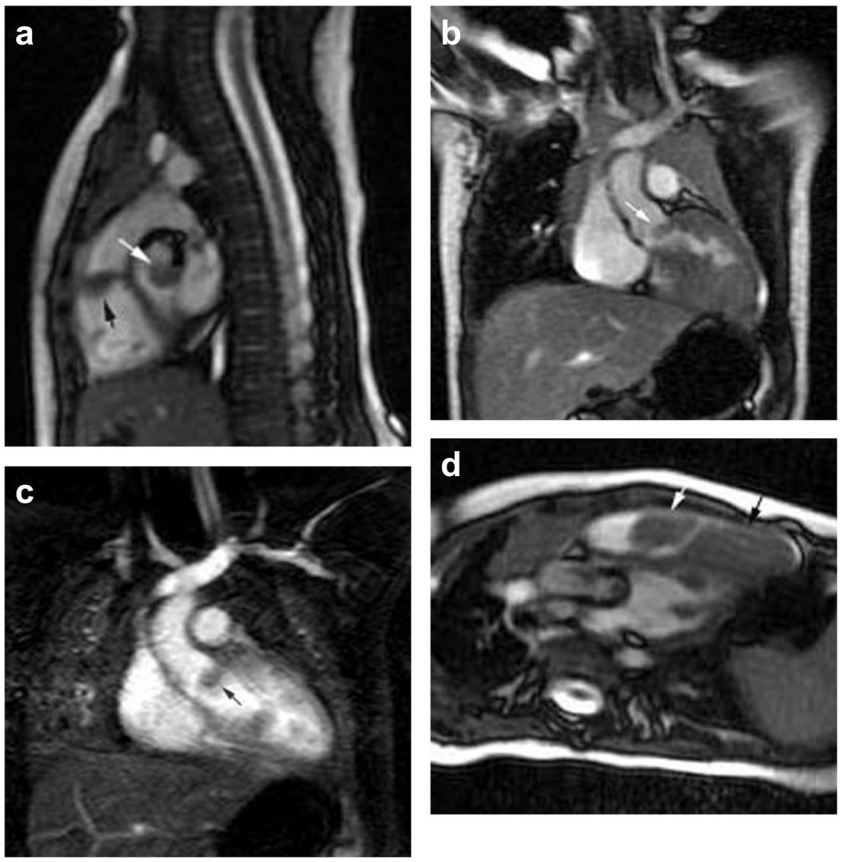

Fig. 4 Cardiac MR images of a boy of Group B at 11 mo; (**a**) A sagittal balanced gradient echo sequence demonstrates a left ventricular outflow tract rhabdomyoma (*white arrow*) and, a right ventricular outflow tract rhabdomyoma (*black arrow*), which lead to outflow tract obstructions; (**b, c**) A coronal balanced gradient echo sequence and CE-MRA reconstructed images display a left ventricular outflow tract rhabdomyoma (*arrows*); (**d**) A transverse balanced gradient echo sequence shows a right ventricular septum rhabdomyoma (*black arrow*) and, a right ventricular outflow tract rhabdomyoma (*white arrow*), which lead to outflow tract obstructions

Subependymal nodules and subependymal giant cell astrocytoma continued to represent two separate majors features in 2012 Consensus Conference Criteria. They are observed in 80% and 5–15% respectively of TSC patients and often detected prenatally or at birth [10]. The pathologic finding of cortical tubers is considered to be a type of focal cortical dysplasia, a single area of focal cortical dysplasia or even two can be observed in an individual who does not have TSC, thus, multiple areas of focal cortical dysplasia count only as one major feature and additional clinical features are necessary to establish a definite diagnosis of TSC [10] (Table 4). In the index study, fetal MRI detected multiple brain lesions in all 5 fetuses but US records did not mention it. Moreover, standard MRI confirmed the fetal MRI results after birth. In the present study, the location of brain lesions was not exactly consistent during prenatal and postnatal periods. This may be due to the fact that the field of view (FOV) of fetal MRI is relatively large compared to the size of the fetal head. The small size of the structure being imaged and the large distance between the fetus and the receiver coil may prevent visualization of small details. During the postnatal period, with the help of scarce myelination, a great number of brain anomalies can be revealed better in neonates (before 3 mo) than in children older than 6 mo of age by early MRI imaging, as they are hyperintense on T1-weighted images and hypointense on T2-weighted images as opposed to the reverse signal intensity in older patients [22]. Furthermore, follow-up MRI should also be performed for those patients with progressive neurological symptoms for several years, ideally to the end of puberty.

In the index study, there is no significant difference between number of brain and/or cardiac lesions detected with pre and postnatal MRI. Also there are technical limitations on Fetal MRI. Fast protocols represent a compromise but they have an important limit about contrast, temporal and spatial resolution. So in index study, authors defined the prenatal brain lesion numbers as “more than” detectable lesions. Actually, cortical and subependimal nodules have not been previously described before second-trimester of gestation on images [23]. On T1 weighted fetal MR images, lesions are generally hyperintense, helping to distinguish them from normal brain tissue. The evaluation of small (<5 mm) rhabdomyomas is difficult due to low contrast and spatial resolution, but cardiac lesion signal analysis may contribute to the study of the fetal heart. Steady State free procession can recognize the nodules as isointense to hypointense signals.

However, the index study was limited by the small number of cases included. Within 20 y of infantile and 11 y of fetal study period, authors collected five fetuses with pre and

Table 4 Clinical diagnostic criteria for both prenatal and postnatal diagnosis of TSC

Features	Prenatal	Postnatal
Major features	A. Brain structure, tubers, and tumors:	A. Dermatology and dentistry:
	1. Subependymal nodules	1. Hypomelanotic macules (≥3, at least 5 mm diameter)
	2. Subependymal giant cell astrocytoma	2. Angiofibromas (≥3) or fibrous cephalic plaque
	3. Cortical dysplasia and white matter lesions	3. Ungual fibromas (≥2)
	B. Cardiology:	4. Shagreen patch
	4. Cardiac rhabdomyoma	B. Ophthalmology:
		5. Multiple retinal hamartomas
		C. Brain structure, tubers, and tumors:
		6. Cortical dysplasias
		7. Subependymal nodules
		8. Subependymal giant cell astrocytoma
		D. Cardiology:
		9. Cardiac rhabdomyoma
		E. Pulmonology:
		10. Lymphangioleiomyomatosis(LAM) *
		F. Nephrology or Liver:
		11. Angiomyolipomas (≥2) *
Minor features		A. Dermatology and dentistry
		1. "Confetti" skin lesions
		2. Dental enamel pits (≥3)
		3. Intraoral fibromas (≥2)
		B. Ophthalmology:
		4. Retinal achromic patch
		C. Nephrology:
		5. Multiple renal cysts
		D. Endocrinology:
		6. Nonrenal hamartomas
Cut-off criteria	Definite diagnosis: Two major features (1 and/or 2 and/or 3 + 4)	Definite diagnosis: Two major features or one major feature with ≥2 minor features
		Probable diagnosis: Either one major feature or ≥2 minor features

*When angiomyolipomas and LAM are both present in a patient with suspected TSC, together they constitute only one major criterion

postnatal MRI exams, 10 infants are postnatal exams in the interest of clarity. The number of fetuses was 50% of that of infants. This may be due to the rarity of the condition prenatally or prenatal findings. Antenatal examination is not required in authors' jurisdiction. And during the fetal period, there may be no symptoms in the fetus leading to further examination such as MRI. However, progressive neurological symptoms may appear after birth, some may be life-threatening. When prenatal echocardiography suggests cardiac rhabdomyomas, authors strongly suggest that fetal MRI should be recommended for further assessment. Thus with early diagnosis of TSC one can give as much information as possible to parents for their decision-making process.

Conclusions

Rhabdomyomas in fetal period are one of the major features of TSC in the Clinical Diagnostic Criteria. This finding alone is not diagnostic of TSC. The presence of both rhabdomyomas and additional findings are consistent with tuberous sclerosis complex. The ability of fetal MRI, as opposed to fetal US, to find cardiac rhabdomyomas and other major features, *i.e.* either cortical tubers (dysplasias) or subependymal nodules, means that a minimum of two Clinical Diagnostic Criteria can be found and the definite diagnosis of TSC can be made in the prenatal period. The authors therefore considered that fetal MRI should become an ideal component of early fetal diagnostic workup in suspected TSC.

Acknowledgements The authors are grateful to their adviser Dr. Steven Saris for reading the manuscript and making many valuable suggestions and revision for improvement.

Contributions All of the MR images were reviewed cooperatively by three radiologists (YZ, SZD and YMZ). The specialties of these three evaluating radiologists are all fetal and pediatric imaging diagnosis, they have dedicated to this field for more than 10 to 20 y. The clinical manifestations and US results were reviewed and discussed at the time of acquisition and when the MR images were interpreted. AMS helped to identify the cardiac lesions of each case. Professor Ming Zhu, a Chinese famous pediatric radiologist, he has studied fetal MRI for more than 10 y; he can take a responsibility that the facts and figures given in the manuscript are true and the article is not under consideration by any other Journal / is not duplicate publication.

Compliance with Ethical Standards

Conflict of Interest None.

Source of Funding National Natural Science Foundation of China (81101032): Fetal MRI combined with 1H MRS quantitative assessment of fetal lung development and oligohydramnios complicated with pulmonary dysplasia National Natural Science Foundation of China (81571628): The diagnosis of fetal congenital heart disease based on the precise qualitative and quantitative MRI scanning technology.

References

1. Ajay V, Singhal V, Venkateshwarlu V, Rajesh SM. Tuberous sclerosis with rhabdomyoma. Indian J Hum Genet. 2013;19:93–5.
2. Jahagirdar PB, Eeraveni R, Ponnuraj S, Kamarthi N. Tuberous sclerosis: a novel approach todiagnosis. J Indian Soc Pedod Prev Dent. 2011;29:S52–5.
3. Colosi E, Russo C, Macaluso G, et al. Sonographic diagnosis of fetal cardiac rhabdomyomas and cerebral tubers: a case report of prenatal tuberous sclerosis. J Prenat Med. 2013;7:51–5.
4. Ozeren S, Cakiroglu Y, Doger E, Caliskan E. Sonographic diagnosis of fetal cardiac rhabdomyomas in two successive pregnancies in a woman with tuberous sclerosis. J Clin Ultrasound. 2012;40:179–82.
5. Sciacca P, Giacchi V, Mattia C, et al. Rhabdomyomas and tuberous sclerosis complex: our experience in 33 cases. BMC Cardiovasc Disord. 2014;14:66.
6. Chen CP, Chang TY, Guo WY, et al. Detection of maternal transmission of a splicing mutation in the TSC2 gene following prenatal diagnosis of fetal cardiac rhabdomyomas mimicking congenital cystic adenomatoid malformation of lung and cerebral tubers and awareness of a family history of maternal epilepsy. Taiwan J Obstet Gynecol. 2013;52:415–9.
7. Gedikbasi A, Oztarhan K, Ulker V, et al. Prenatal sonographic diagnosis of tuberous sclerosis complex. J Clin Ultrasound. 2011;39:427–30.
8. Charif DOuazzane M, Gueroui I, Betaich K, et al. A cardiac rhabdomyome evoking the antenatal diagnosis of a Bourneville's tuberous sclerosis. Ann Cardiol Angeiol. 2015;64:51–3.
9. Falip C, Hornoy P, Millischer Bellaïche AE, et al. Fetal cerebral magnetic resonance imaging (MRI). Indications, normal and pathological patterns. Rev Neurol. 2009;165:875–88.
10. Northrup H, Krueger DA; International tuberous sclerosis complex consensus group. Tuberous sclerosis complex diagnostic criteria update: recommendations of the 2012 international tuberous sclerosis complex consensus conference. Pediatr Neurol. 2013;49:243–54.
11. Muhler MR, Rake A, Schwabe M, et al. Value of fetal cerebral MRI in sonographically proven cardiac rhabdomyoma. Pediatric Radiol. 2007;37:467.
12. Islam MP, Roach ES. Neurocutaneous syndromes. In: Daroff RB, Fenichel GM, Jankovic J, Mazziotta J, editors. Bradley's Neurology in Clinical Practice, vol. II. 6th ed. Saunders: Elsevier; 2012. p. 1508–33.
13. Haines JL, Amos J, Attwood J, et al. Genetic heterogeneity in tuberous sclerosis. Study of a large collaborative dataset. Ann N Y Acad Sci. 1991;615:256–64.
14. Penha JG, Zorzanelli L, Barbosa-Lopes AA, et al. Heart neoplasms in children: retrospective analysis. Arq Bras Cardiol. 2013;100:120–6.
15. Gusman M, Servaes S, Feygin T, Degenhardt K, Epelman M. Multimodal imaging in the prenatal diagnosis of tuberous sclerosis complex. Case Rep Pediatr. 2012;2012:925646.
16. Kocabas A, Ekici F, Cetin İİ, et al. Cardiac rhabdomyomas associated with tuberous sclerosis complex in 11 children: presentation to outcome. Pediatr Hematol Oncol. 2013;30:71–9.
17. Pruksanusak N, Suntharasaj T, Suwanrath C, et al. Fetal cardiac rhabdomyoma with hydrops fetalis: report of 2 cases and literature review. J Ultrasound Med. 2012;31:1821–4.
18. Hoshal SG, Samuel BP, Schneider JR, Mammen L, Vettukattil JJ. Regression of massive cardiac rhabdomyoma on everolimus therapy. Pediatr Int. 2016;58:397–9.
19. Gamzu R, Achiron R, Hegesh J, et al. Evaluating the risk of tuberous sclerosis in cases with prenatal diagnosis of cardiac rhabdomyoma. Prenat Diagn. 2002;22:1044–7.
20. Kivelitz DE, Muhler M, Rake A, et al. MRI of cardiac rhabdomyoma in the fetus. Eur Radiol. 2004;14:1513–6.
21. de Laveaucoupet J, Bekiesińska-Figatowska M, Rutkowska M. What is the impact of fetal magnetic resonance imaging (MRI) on prenatal diagnosis of cerebral anomalies. Med Wieku Rozwoj. 2011;15:376–84.
22. Baron Y, Barkovich A. MR imaging of tuberous sclerosis in neonates and young infants. AJNR. 1999;20:907–16.
23. Levine D, Barnes P, Korf B, et al. Tuberous sclerosis in the fetus: second trimester diagnosis of subependymal with ultrafast MR imaging. AJR Am J Roentgenol. 2000;175:1067–9.